

# Journal of Hunan University (Natural Sciences)

Vol. 53 No. 3

March 2026

Available online at

<https://jonuns.com>



ELSEVIER  
Scopus



Clarivate  
WEB OF SCIENCE

Open Access Article

 <https://doi.org/10.55463/issn.1674-2974.53.3.12>

## Cellulose-Fiber Based Biomaterial from Sengon (*Paraserianthes falcataria*) Bark Waste for Slow-released Perfumery Patchouli Oil

Masruri MASRURI<sup>1\*</sup>, Alyaa Farah Dibha<sup>1</sup>, Elvira Nuravida<sup>1</sup>, Adam Wiryawan<sup>1</sup>, Nur Ikhtiarini<sup>2</sup>,  
I Wayan Karta<sup>3</sup>, Hendrix Yulis Setyawan<sup>4</sup>, Firda Aulya Syamani<sup>5</sup>

<sup>1</sup> Chemistry Department, Faculty of Mathematics and Natural Sciences, Brawijaya University, Malang 65145, Indonesia,

<sup>2</sup> Chemical Engineering Department, Faculty of Engineering and Science, Universitas Pembangunan Nasional "Veteran" Jawa Timur, Surabaya 60294, Indonesia,

<sup>3</sup> Department of Medical Laboratory Technology, Poltekkes Kemenkes Denpasar, Denpasar, Indonesia,

<sup>4</sup> Department of Agricultural Industry Technology, Faculty of Agricultural Technology, Brawijaya University, Indonesia,

<sup>5</sup> Research Center for Biomass and Bioproducts, National Research and Innovation Agency (BRIN), Tangerang Selatan 15314, Indonesia,

\* Corresponding author: [masruri@ub.ac.id](mailto:masruri@ub.ac.id)

### Article History:

Received: February 5, 2026

Revised: March 16, 2026

Accepted: March 24, 2026

Published: March 31, 2026

**Abstract:** Sengon (*Paraserianthes falcataria*) bark, an abundant lignocellulosic biomass waste in Indonesia, was utilized as a renewable precursor for the development of cellulose-based biomembranes. Cellulose fibers were isolated and chemically modified using urea and epichlorohydrin (ECH) to fabricate cross-linked three-dimensional biomembranes for essential oil storage and controlled-release applications.

The isolated cellulose appeared as fine pale-white fibers with a crystallinity index of 34.6%, indicating a predominantly amorphous structure. Fourier-transform infrared (FTIR) spectroscopy confirmed characteristic cellulose peaks at 3350 and 1000  $\text{cm}^{-1}$ , while a weak band at 1650  $\text{cm}^{-1}$  suggested the presence of residual lignin. Increasing ECH concentration resulted in smoother and denser membrane morphologies, as observed by scanning



Copyright: © 2026 by the authors. Licensee JHU

This article is an open-access article distributed under the terms and conditions of the Creative Commons Attribution License (<http://creativecommons.org/licenses/by/4.0/>)

electron microscopy (SEM), indicating enhanced cross-linking density. FTIR spectra of the modified biomembranes further revealed the emergence of N–H and C–N stretching bands, confirming successful chemical modification.

The unmodified membrane (CFM0) exhibited the highest patchouli essential oil loading capacity (24.7 mg/cm<sup>2</sup>), whereas commercial filter paper showed the lowest capacity (10.1 mg/cm<sup>2</sup>). Increasing ECH concentration reduced oil loading capacity but significantly improved controlled-release behavior.

Overall, cellulose biomembranes derived from sengon bark demonstrate strong potential as a sustainable and tunable platform for essential oil encapsulation and controlled-release systems.

**Keywords:** Cellulose; Biomembrane; Lignocellulosic biomass; Cross-linking; Essential oil encapsulation; Controlled release.

## 基于木豆树 (*Paraserianthes falcataria*) 树皮废弃物的纤维素纤维生物材料用于广藿香精油的缓释释放

**摘要:** 印尼丰富的木豆树 (*Paraserianthes falcataria*) 树皮作为一种重要的木质纤维素生物质废弃物, 被用作开发纤维素基生物膜的可再生原料。通过分离纤维素纤维, 并利用尿素和环氧氯丙烷 (ECH) 进行化学改性, 制备了交联的三维生物膜, 用于精油的储存与控释应用。

所得纤维素呈细小的浅白色纤维状, 其结晶度为34.6%, 表明其以非晶结构为主。傅里叶变换红外光谱 (FTIR) 在3350 cm<sup>-1</sup>和1000 cm<sup>-1</sup>处显示出典型的纤维素特征吸收峰, 而1650 cm<sup>-1</sup>处的弱吸收带表明存在少量残余木质素。随着ECH浓度的增加, 扫描电子显微镜 (SEM) 观察到膜表面更加光滑致密, 说明交联程度增强。改性生物膜的FTIR光谱中出现了新的N-H和C-N伸缩振动峰, 进一步证实了化学改性的成功。

未改性膜 (CFM0) 表现出最高的广藿香精油负载能力 (24.7 mg/cm<sup>2</sup>), 而商业滤纸的负载能力最低 (10.1 mg/cm<sup>2</sup>)。随着ECH浓度的增加, 精油负载能力有所降低, 但控释性能显著提升。

总体而言, 来源于木豆树树皮的纤维素生物膜在精油包埋与控释体系中展现出良好的应用潜力, 是一种可持续且可调控的功能材料平台。

**关键词:** 纤维素; 生物膜; 木质纤维素生物质; 交联; 精油包埋; 控释系统

### 1. Introduction

Biomass waste is often perceived as valueless byproduct, however it possesses significant potential to be utilized as a sustainable solution in the modern era [1]. Among the various types of biomass waste abundantly available in Indonesia, Sengon (*Paraserianthes falcataria*) bark stands out as a major byproduct of the timber industry that is frequently discarded or left unutilized [2]. The Sengon tree is widely distributed throughout Indonesia and is highly valued for its versatility, being extensively employed in timber production, packaging materials, and furniture manufacturing [3]. Furthermore, Sengon wood waste has been successfully converted into cellulose and

subsequently synthesized into antibacterial hydrogels [4].

Cellulose is one of the most abundant natural biomolecular polymers [5], a renewable and biodegradable [6], and can be isolated from agricultural [7], [8] and forestry biomass waste [9], [10]. Cellulose is a glucose-based polymer composed of numerous  $\beta$ -1,4-linked D-glucose subunits held together by glycosidic linkages, van der Waals forces, and hydrogen bonds [11]. Each cellulose chain consist of repeating glucose units, and every glucose residue contains three hydroxyl groups (-OH) which are located at the equatorial position of the glucose ring [12]. Due to its structural characteristics, cellulose has been extensively

utilized as a biomembrane [13], often fabricated in the form of porous, sponge-like matrices or thin multilayer films for the storage and controlled release of bioactive compounds [14,15]. For membrane or cavity formation, cross-linking is required to establish a stable three-dimensional network. This process involves the interweaving of bonds between polymer chains, which can be either hydrogen or covalent in nature. When cross-linking occurs through hydrogen bonding, a reagent or cross-linker containing electron-deficient hydrogen atoms is typically needed [16,17]. Commonly used reagents and cross-linker include urea [18], citric acid [19,20], various dicarboxylic acid, and several inorganic bases such as calcium hydroxide, phosphoric acid, and zinc hydroxide.

However, the formation of crosslink does not necessarily occur easily. Cross-linkers capable of forming covalent bonds, known for their bond strength, include glutaraldehyde [21,22], epichlorohydrin [23], epoxides of ethylene glycol and poly vinyl alcohol [24] as well as several other diester-based reagents. The molecular size of the cross-linker significantly influences the pore size during the formation of porous or cavity-type biomembranes [25,26]. Furthermore, the number and reactivity of cross-linkers also affect the morphology of the resulting biomembrane, determining whether it develops as a two-dimensional (2D) or three-dimensional (3D) structure. Higher cross-linker reactivity generally leads to the formation of a greater number of smaller pores, and in some cases, promotes the development of extended three-dimensional porous networks.

Despite extensive studies on cellulose-based biomaterials, limited research has focused on utilizing Sengon (*Paraserianthes falcataria*) bark as a cellulose source for the fabrication of cross-linked 3D biomembranes. Moreover, comparative studies on the use of urea and epichlorohydrin as dual cross-linkers for essential oil encapsulation are still scarce. Previous cellulose-based biomaterials that commonly rely on single cross-linkers and widely used biomass sources. Therefore, this study introduces a novel approach by utilizing Sengon bark, an underexplored lignocellulosic biomass, as a cellulose source combined with a dual cross-linking system using urea and epichlorohydrin. The developed three-dimensional biomembrane capable of controlled essential oil release. The findings are expected to provide new insights into the valorization of lignocellulosic waste and contribute to the advancement of sustainable biomaterials for pharmaceutical and biomedical applications.

## 2. Materials and Method

### 2.1 Materials

Materials used in this study include Sengon (*Paraserianthes falcataria*) bark was collected from a local farmer in Malang, East Java, Indonesia. The bark

was thoroughly cleaned with distilled water, dried at room temperature, and cut into piece approximately 10 cm in lengths. The chemicals used were sodium hypochlorite (NaOCl), sodium hydroxide (NaOH, Merck), urea ((NH<sub>2</sub>)<sub>2</sub>CO, Merck), epichlorohydrin (C<sub>3</sub>H<sub>5</sub>ClO, ECH, Sigma-Aldrich), and essential oils (patchouli oil). The instrumentation used include fourier transform infrared spectroscopy (FTIR, Shimadzu 8400s), UV-Visible spectrophotometer (Shimadzu UV-1601), Scanning Electron Microscope (FESEM Quanta FEG 650), and X-Ray Diffraction (XRD, PANalytical X'pert-PRO).

### 2.2 Procedure

#### 2.1.1. Cellulose fiber (CF) isolation

A total of 1 kg of sengon bark was soaked with NaOH (6%) (1:10 ratio) for 24 hours. Soaking was done for 2 times. The results of soaking with NaOH were then soaked with 12% NaOCl (1:10) for 24 hours at 80 °C. The bleaching process was carried out until the fiber was white. The bleaching results were then neutralized with distilled water until the pH was neutral (pH = 7). The cellulose fibers obtained were then oven dried at 80 °C. Cellulose fibers were obtained with a yield of 7.4%.

#### 2.1.2. Biomaterials fabrication

Three-dimensional (3D) material was prepared by dissolving urea in distilled water, followed by the addition of sengon bark cellulose fiber (CF). The mixture was stirred at 300 rpm for 3 hours at room temperature. Then ECH was added under room temperature at 100 rpm for 30 minutes. The resulting suspension was then poured into a mould with dimensions of 5 x 6 cm, dried under ambient conditions, and subsequently vacuum-dried in a desiccator to remove residual moisture.

**Table 1.** Concentration of Biomaterials constituents

Sample code	Cellulose fiber (g)	Urea (g)	Distilled water (mL)	ECH (μL)
CFM0	0.4	2	8	0
CFM4	0.4	2	8	400
CFM6	0.4	2	8	600
CFM8	0.4	2	8	800

#### 2.1.3. Characterization

##### 1) Fourier Transform Infrared (FTIR) Spectroscopy analysis

FTIR spectra were recorded based on smart iTX-Diamond fitted with an ATR (attenuated total reflectance) system. Spectra were collected in the range of 500-4000 cm<sup>-1</sup> with a resolution of 4 cm<sup>-1</sup> and accumulation of 10 scan. Samples were prepared in powder form and then placed directly onto the ATR

crystal. All measurements were conducted at room temperature.

## 2) Scanning Electron Microscopy observation

The morphology of cellulose fibre and biomaterial (thickness and surface morphology) were examined using scanning electron microscopy (SEM). Surface image were obtained with a field emission scanning electron microscope (FESEM Quanta FEG 650, Thermo Fisher Scientific) operated at an accelerating voltage of 5 kV. Prior to imaging, samples were sputter-coated with a thin layer of gold to enhance surface conductivity and image resolution.

## 3) X-Ray Diffractometer analysis

The crystallinity and phase structure of the cellulose fibres and biomaterials were analyzed using X-ray diffraction (XRD). Measurements were performed with a PANalytical X'Pert PRO diffractometer equipped with Cu K $\alpha$  radiation ( $\lambda = 1.5406 \text{ \AA}$ ), operated at 40 kV and 30 mA. Diffraction patterns were recorded over a  $2\theta$  range of  $5^\circ$ - $60^\circ$  with a step size of  $0.02^\circ$  and a scanning rate of  $2^\circ \text{ min}^{-1}$ . The degree of crystallinity ( $CrI$ ) of the cellulose samples was calculated using the Segal method (Equation 1) [27]:

$$CrI (\%) = \frac{I_{200} - I_{am}}{I_{200}} \times 100 \quad 1$$

where  $I_{200}$  represents the intensity of the (200) crystalline peak (typically around  $2\theta = 22^\circ$ ), and  $I_{am}$  is the intensity at the minimum (around  $2\theta = 18^\circ$ ), which corresponds to the amorphous region.

## 4) Patchouli oil loading and release test using UV visible spectrophotometry

The loading of patchouli essential oils into the cellulose-based biomaterial was carried out using the immersion method. Dried biomaterials were immersed in essential oil solutions for 24 h at room temperature to allow for adsorption and diffusion of the oils into the membrane matrix. After loading, the membranes were removed, gently wiped to remove excess surface oil, and dried at ambient conditions for 12 h. The amount of essential oil loaded was determined by the mass difference before and after impregnation, as expressed by Equation 2 [28].

The release process was conducted to evaluate the controlled-release behavior of each biomaterial. The release test was performed by observing the remaining essential oil mass ( $M_m$ ) retained in the biomaterial over time. Measurements were taken every 60 minutes, from 0 to 360 minutes. The release efficiency of essential oil ( $R_{EO}$ ) was calculated using Equation 3 [29]

:

$$Loading\ capacity (\%) = \frac{W_L - W_0}{W_0} \times 100 \quad 2$$

$$R_{EO} (\%) = \frac{SC - (M_S - M_{tn})}{SC} \times 100 \quad 3$$

where  $W_L$  is the weight of the oil-loaded biomaterial and  $W_0$  is the weight of the dry biomaterial before loading.  $SC$  is the initial storage capacity of the essential oil,  $M_S$  is the initial mass of the loaded biomaterial, and  $M_{tn}$  is the mass of essential oil remaining at each time interval  $t_n$

## 3. Result and Discussion

### 3.1. Cellulose Fiber result

The cellulose fibers obtained from Sengon (*Paraserianthes falcataria*) bark appeared physically as pale white, fine fibers (Figure 1A). This colour change from the original brownish bark indicates the partial removal of non-cellulosic components such as lignin, hemicellulose, and other extractives during the isolation process. The fibrous morphology suggests that the mechanical and chemical treatments successfully loosened the fibrous structure, facilitating fibrillation and partial purification of cellulose.

The morphological structure observed by SEM confirmed that the isolated cellulose possessed a fibrous and thread-like texture with relatively smooth surfaces, indicating the effective breakdown of the lignocellulosic matrix. However, the presence of minor agglomerates and surface irregularities may suggest that some non-cellulosic residues, such as lignin or hemicellulose, were still attached to the cellulose surface (Figure 1B).

The XRD analysis revealed a crystallinity index of 34.6%, indicating that the cellulose obtained is predominantly amorphous (figure 1C). This relatively low crystallinity can be attributed to partial disruption of the crystalline regions during the chemical isolation process. Amorphous cellulose structures generally enhance reactivity and flexibility, which are advantageous for further modification and cross-linking in biomaterial synthesis.

FTIR spectra further confirmed the chemical structure of the cellulose fibers (Figure 1D). The characteristic absorption band around  $1000 \text{ cm}^{-1}$  corresponds to C-O-C stretching vibrations of the pyranose ring, confirming the polysaccharide backbone of cellulose. A broad absorption around  $3350 \text{ cm}^{-1}$  is attributed to O-H stretching vibrations of hydroxyl groups, typical of cellulose. However, an additional peak observed near  $1650 \text{ cm}^{-1}$  indicates the presence of aromatic C=C stretching vibrations, suggesting residual lignin within the cellulose structure. The presence of this lignin-related band confirms that the isolated cellulose is not completely pure, which aligns with the relatively low crystallinity index obtained from XRD analysis.

Plant bark has been reported as a potential source of natural cellulose fibers due to its lignocellulosic

composition. Previous studies have shown that bark tissues contain cellulose in fibrous form embedded within lignin and hemicellulose matrices. For instance, cellulose-rich fibers have been successfully extracted from the bark of jack tree (*Artocarpus heterophyllus*) branches, exhibiting low density, high crystallinity, and good thermal stability, confirming that plant bark can serve as a viable source of natural cellulose fibers for various applications [30].

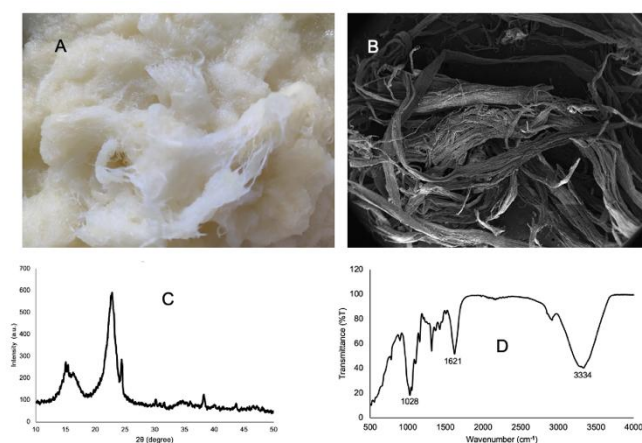


**Figure 1. Cellulose Fiber, CF (A), SEM image (B), XRD Diffractogram, and FTIR spectrum (D) of cellulose fiber**

### 3.2. Biomaterials produced

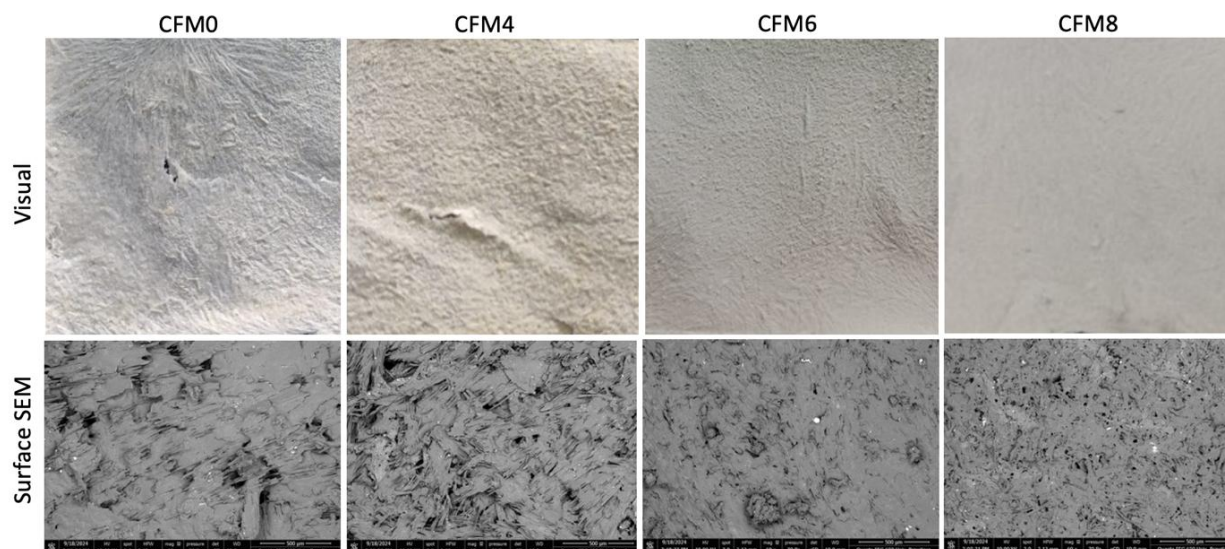


**Figure 2. Biomaterials (1<sup>st</sup> row) and SEM image of surface (2<sup>nd</sup> row)**

Cross-sectional SEM images further supported these findings (Figure 2). The cross-sectional SEM images (Figure a–d) clearly demonstrate the influence of ECH concentration on the internal morphology and thickness of the cellulose-based films. As the amount of ECH increased, noticeable structural changes occurred in the compactness and organization of the polymer matrix. In

Figure 2 showed biomaterials obtained and SEM image (surface and cross section). The produced biomaterials exhibited distinct morphological changes with varying concentrations of epichlorohydrin (ECH) used as the cross-linking agent. Visually, as the ECH concentration increased, the biomaterial surface appeared smoother and more homogeneous. This observation suggests that a higher degree of cross-linking led to a denser polymeric network, reducing surface roughness and porosity. The SEM surface micrographs confirmed this trend, showing a progressive transition from a relatively coarse and irregular surface at lower ECH concentrations to a smoother and more compact morphology at higher concentrations. The increased cross-linking density facilitated stronger intermolecular bonding between cellulose chains, which improved surface uniformity and structural integrity. An increase in cross-linker concentration has been reported to produce smoother and more uniform hydrogel surfaces due to the formation of denser polymer networks. Similar observations were reported by Ikhtiarini et al. (2023), where higher cross-linking density resulted in reduced surface roughness and a more compact hydrogel structure [4]. The presence of fewer voids and smoother textures at higher ECH levels also indicates enhanced polymer compatibility and more efficient cross-link formation throughout the membrane matrix.

the control sample (CFM0), the structure appeared loosely arranged with irregular layers, indicating that the cellulose chains were not yet effectively cross-linked. This resulted in a relatively open structure with visible interstitial spaces. When a moderate amount of ECH was introduced (CFM4), the structure became more compact and cohesive, suggesting the initiation of

intermolecular bonding between adjacent cellulose hydroxyl groups through the bifunctional epoxide groups of ECH. At an even higher cross-linker concentration (CFM6), the internal structure exhibited a denser and more uniform arrangement with reduced voids. This morphological feature reflects the formation of a more organized three-dimensional cross-linked network, which effectively compacts the polymer chains and results in a decrease in film thickness. However, further increasing the ECH concentration (CFM8), produced an opposite trend. The cross-section revealed a less compact and swollen morphology, likely due to excessive cross-linking or uneven distribution of ECH within the matrix. This over-cross-linking can induce internal stress or swelling of the polymer network, leading to an increase in thickness [31].

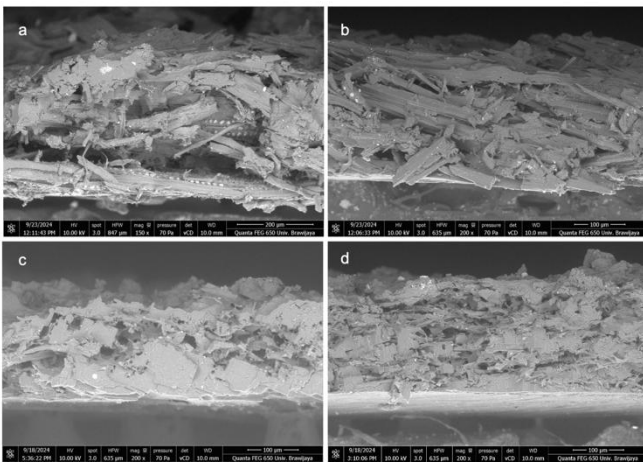


**Figure 3.** Cross-section SEM image of a) CFM0, b) CFM4, c) CFM6, and d) CFM8 biomaterials

**Table 2.** The thickness of biomaterials

Sample	Thickness ( $\mu\text{m}$ )
CFM0	193.90
CFM4	197.67
CFM6	176.76
CFM8	223.26

The FTIR spectra (Figure 4) and the corresponding functional group assignments (Table 3) reveal clear structural differences between the cellulose fibres (CF) and the modified biomaterials (CFM0, CFM4, CFM6, and CFM8). These variations confirm the successful chemical modification and cross-linking reactions involving urea and epichlorohydrin (ECH). A broad absorption at  $3327\text{ cm}^{-1}$  corresponds to O–H stretching, indicating that the cellulose backbone remained intact, while its broadness in the modified membranes suggests enhanced hydrogen bonding among cellulose, urea, and ECH. New bands at  $3427\text{ cm}^{-1}$  (N–H stretching) and  $1672\text{ cm}^{-1}$  (N–H deformation), absent in the unmodified cellulose (CF), verify the incorporation of nitrogen-containing groups from urea. The appearance of the C–N stretching band at  $1461\text{ cm}^{-1}$  further confirms the formation of chemical linkages involving nitrogen, supporting the success of the cross-linking process. Bands at  $1153\text{--}1036\text{ cm}^{-1}$  (C–O stretching) and near  $1000\text{ cm}^{-1}$  (pyranose ring vibration) demonstrate that the cellulose structure was preserved after modification. Meanwhile, a minor peak around  $1650\text{ cm}^{-1}$  suggests residual lignin, indicating that the cellulose fibres were not fully purified.

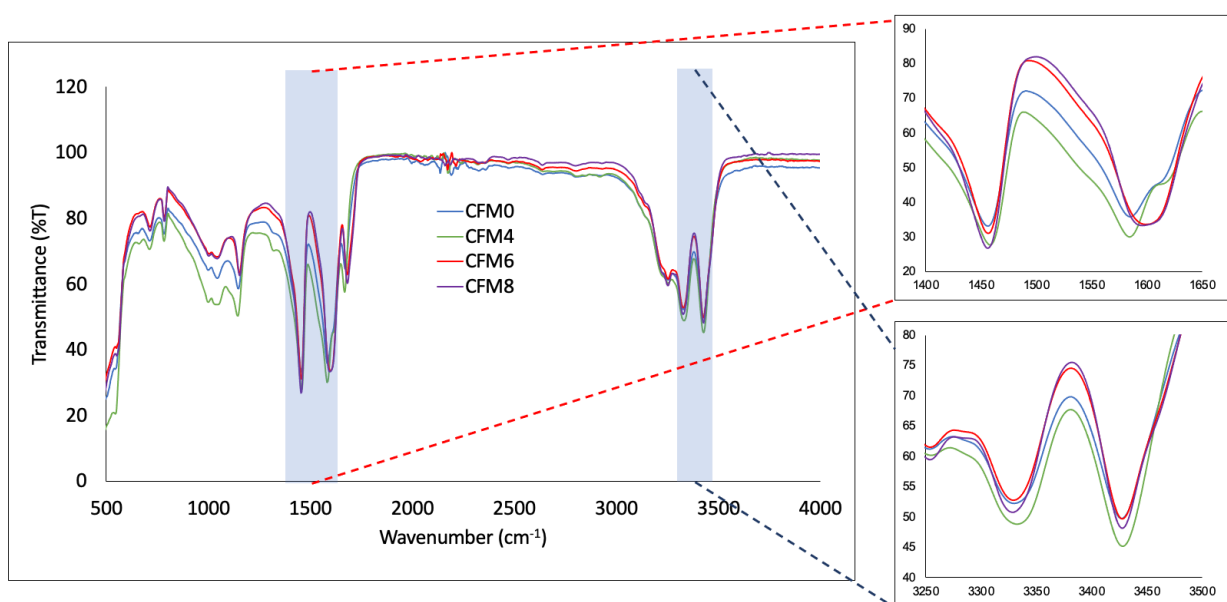


**Figure 4.** FTIR spectra of biomaterials

**Table 3. Absorption peak that appears on biomaterials**

Wave number (cm <sup>-1</sup> )	Functional group/assignment	CF	CF M0	CF M4	CF M6	CF M8
3427	N-H stretch	-	√	√	√	√
3327	Hydroxy group, H-bonded OH stretch	√	√	√	√	√
1672	C=C vibration	√	√	√	√	√
1617-1578	OH-bending of adsorbed water	√	√	√	√	√
1461	C-N stretching	-	√	√	√	√
1153-1036	C-O stretching	√	√	√	√	√

Figure 5A illustrates the storage capacity of patchouli essential oil in the cellulose-based biomaterials prepared with different ECH concentrations, compared to commercial filter paper (FPC) as a reference. The FPC exhibited the lowest storage capacity (10.1 mg/cm<sup>2</sup>), indicating its limited ability to retain essential oil due to the absence of chemical modification and cross-linked structure. In contrast, the unmodified cellulose membrane (CFM0) showed the highest storage capacity (24.7 mg/cm<sup>2</sup>), more than twice that of FPC. This improvement is attributed to the presence of urea-derived functional groups that enhanced hydrogen bonding and dipole interactions with the polar constituents of patchouli oil. The incorporation of urea likely increased the membrane's hydrophilicity and surface affinity, promoting higher oil adsorption. As the ECH concentration increased (CFM4-CFM8), the storage capacity gradually decreased to 17.5-15.2 mg/cm<sup>2</sup>. This trend indicates that higher degrees of cross-linking led to denser polymer networks, which reduced pore volume and limited the availability of active binding sites. While ECH strengthens the membrane structure, excessive cross-linking can restrict the diffusion and absorption of oil molecules into the matrix.

The release profiles in Figure 5B further support these observations. The commercial filter paper (FPC) released oil rapidly, reaching over 80% within the first 120 minutes, while the modified membranes exhibited progressively slower release rates with increasing ECH

concentration. Samples CFM6 and CFM8 demonstrated the most controlled release behavior, reflecting the influence of a more compact and ordered internal structure formed by extensive cross-linking.

The effect of cross-linking density on the oil loading capacity and release behavior can be further understood from a structural perspective [32]. The polymer network gets more densely packed as cross-linking density rises, which results in a decrease in pore size and total free volume. Therefore, the loading drops of oil because there is not enough room for the molecules to get trapped inside. The mass transfer mechanism is greatly impacted by the constrained pore configuration. The diffusion channel becomes more convoluted in strongly cross-linked systems, impeding the mobility of encapsulated oil molecules. Consequently, a diffusion-controlled mechanism with a lower release rate controls the release process. This behavior is in line with normal polymeric delivery methods, where improved barrier qualities result from greater network rigidity.

Furthermore, the preservation of oil molecules may be facilitated by increased intermolecular interactions inside the thick polymer network. The encapsulated phase may be stabilized by these interactions, further postponing its release. Therefore, depending on the intended use, an ideal cross-linking density is needed to strike a balance between adequate loading capacity and desired controlled release characteristics.

A comparison with previously reported cellulose-based materials reveals that the behavior observed in this study is consistent with general trends in polymeric delivery systems. Several studies have reported that increasing cross-linking density in cellulose-derived matrices leads to reduced loading capacity due to decreased free volume and pore accessibility [33,34]. Similar findings have been observed in modified cellulose hydrogels and nanocellulose-based carriers, where tighter network structures limit the incorporation of hydrophobic compounds such as essential oils [35].

The cross-linked cellulose-based polymer that was created has encouraging potential for real-world uses, especially in controlled release systems. It is appropriate for usage in industries including food packaging, medicines, and agricultural formulations due to its capacity to modify oil loading and release behavior by adjustment of cross-linking density. For example, the material might be used in active food packaging to release antimicrobial essential oils gradually, increasing the shelf life of the product. In a similar vein, it might operate as a carrier for bioactive substances that need to be released gradually in medicinal applications.

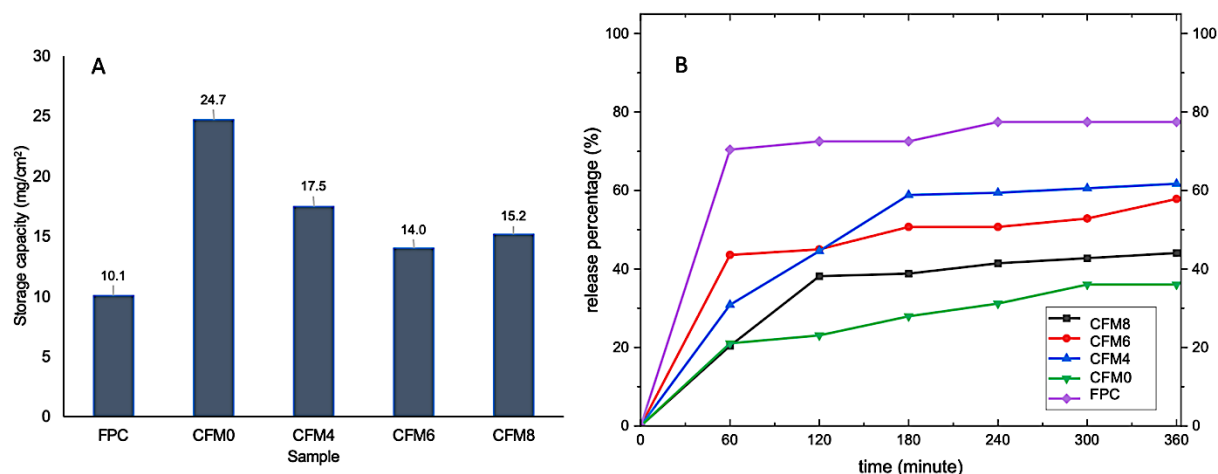


**Figure 5. Storage capacity (A) and release percentage (B) of biomaterials to Patchouli essential oil compared to filter paper commercial (CFM)**

#### 4. Conclusion

Cellulose fibers were successfully isolated from *Sengon* (*Paraserianthes falcataria*) bark, appearing as fine pale-white fibers. SEM confirmed their fibrillar morphology, while XRD analysis showed a crystallinity index of 34.6%, indicating a predominantly amorphous structure. FTIR spectra displayed characteristic cellulose peaks at around  $1000\text{ cm}^{-1}$  (pyranose ring) and  $3350\text{ cm}^{-1}$  (hydroxyl group), with a weak band at  $1650\text{ cm}^{-1}$  indicating residual lignin, suggesting incomplete purification. The cellulose fibers were modified using urea and various concentrations of epichlorohydrin (ECH) to form cross-linked 3D biomaterials. Visual and SEM observations revealed that increasing ECH concentration produced smoother and denser membrane surfaces, confirming more compact polymer arrangements. FTIR analysis showed new absorption bands associated with N-H stretching ( $3427\text{ cm}^{-1}$ ), C-N stretching ( $1461\text{ cm}^{-1}$ ), and C-O stretching ( $1153\text{--}1036\text{ cm}^{-1}$ ), confirming successful cross-linking. Patchouli essential oil storage and release tests showed that the unmodified membrane (CFM0) exhibited the highest storage capacity ( $24.7\text{ mg/cm}^2$ ), while commercial filter paper (FPC) had the lowest ( $10.1\text{ mg/cm}^2$ ). However, higher ECH concentrations led to decreased storage but improved controlled-release behavior due to denser network formation. These results indicate a balance between high loading capacity and sustained release can be achieved under moderate cross-linking.

Future research should concentrate on testing a larger variety of essential oils with various physicochemical characteristics in order to increase the produced usefulness of materials. To assess its practical viability, additional research on long-term stability, including storage conditions and structural endurance, is required. Examining the synthesis scalability of process and performance in actual application scenarios would also

yield insightful information for possible industrial application.

#### Acknowledgement

This research is fund by Penelitian Dasar Unggulan Perguruan Tinggi (PDUPT) of Brawijaya University year 2024 number 00140.12/UN10.A0501/B/PT.01.03.2/2024.

#### Declaration statement

There are no competing interest for this submission.

#### References

- [1] M. Casau, M. F. Dias, J. C. O. Matias, and L. J. R. Nunes, "Residual Biomass: A Comprehensive Review on the Importance, Uses and Potential in a Circular Bioeconomy Approach," *Resources*, vol. 11, no. 4, pp. 1–16, 2022, doi: 10.3390/resources11040035. <https://doi.org/10.3390/resources11040035>
- [2] A. Haryanto, S. Triyono, D. Wulandari, M. R. Ridho, C. W. Purnomo, "Valorization of Indonesian wood wastes through pyrolysis: A review," *Energies*, vol. 14, no. 5, pp. 1–25, 2021, doi: 10.3390/en14051407. <https://doi.org/10.3390/en14051407>
- [3] I. Rahayu, F. C. Dirna, A. Maddu, W. Darmawan, D. Nandika, and E. Prihatini, "Dimensional stability of treated sengon wood by nano-silica of betung bamboo leaves," *Forests*, vol. 12, no. 11, pp. 1–9, 2021, doi: 10.3390/f12111581. <https://doi.org/10.3390/f12111581>
- [4] N. Ikhtiarini, M. Masruri, S. M. Ulfa, R. Rollando, and N. Widodo, "Antibacterial Activity of Hydrogels Produced from Nanocellulose Derivatives for Controlled Drug Delivery," *Tropical Journal of Natural Product Research (TJNPR)*, vol. 8, no. 5, Art. no. 5, May

- 2024, doi: 10.26538/tjnpr/v8i5.3  
<https://doi.org/10.26538/tjnpr/v8i5.3>
- [5] S. Magalhães, A. Ferreira, F. Silva, J. Teixeira, C. M. R. Rocha., “Eco-Friendly Methods for Extraction and Modification of Cellulose: An Overview,” *Polymers*, vol. 15, no. 14, pp. 1–25, 2023, doi: 10.3390/polym15143138.  
<https://doi.org/10.3390/polym15143138>
- [6] N. Ikhtiarini, M. Masruri, S. M. Ulfa, W. Widodo, “Biocompatible composites based on alginate, polycaprolactone, and nanocellulose - A review,” *International Journal of Biological Macromolecules*, vol. 311, p. 143423, Jun. 2025, doi: 10.1016/j.ijbiomac.2025.143423.  
<https://doi.org/10.1016/j.ijbiomac.2025.143423>.
- [7] R. S. Abolore, S. Jaiswal, and A. K. Jaiswal, “Green and sustainable pretreatment methods for cellulose extraction from lignocellulosic biomass and its applications: A review,” *Carbohydrate Polymer Technologies and Applications*, vol. 7, no. November 2023, p. 100396, 2024, doi: 10.1016/j.carpta.2023.100396.  
<https://doi.org/10.1016/j.carpta.2023.100396>
- [8] L. K. Latif, M. Masruri, and B. Rumhayati, “A Potency of Microcellulose from Pineapple Leave Isolated by Hydrolysis-Assisted Sonication,” *IOP Conference Series: Materials Science and Engineering*, vol. 833, no. 1, 2020, doi: 10.1088/1757-899X/833/1/012020. <https://doi.org/10.1088/1757-899X/833/1/012020>.
- [9] M. Masruri, F. R. Azizah, N. Ikhtiarini, A. Srihardyastutie, and Moh. F. Rahman, “Characterization of microcrystalline cellulose derived from pinewood waste (*Pinus merkusii*) hydrolyzed with hydrochloric acid,” *AIP Conference Proceedings*, vol. 2818, no. 1, p. 80002, Aug. 2023, doi: 10.1063/5.0131197.  
<https://doi.org/10.1063/5.0131197>
- [10] S. Plakantonaki, A.N. Papadopoulos, H. R. Taghiyari, E. T. Athanassiadou, I. Kakaras, “Investigating the Routes to Produce Cellulose Fibers from Agro-Waste: An Upcycling Process,” *ChemEngineering*, vol. 8, no. 6, pp. 1–32, 2024. <https://www.mdpi.com/2305-7084/8/6/112>
- [11] J. A. Okolie, S. Nanda, A. K. Dalai, and J. A. Kozinski, “Chemistry and Specialty Industrial Applications of Lignocellulosic Biomass,” *Waste and Biomass Valorization*, vol. 12, no. 5, pp. 2145–2169, 2021, doi: 10.1007/s12649-020-01123-0.  
<https://doi.org/10.1007/s12649-020-01123-0>
- [12] L. Bourassi, M. El Achaby, M. Bousmina, A. E. K. Qaiss, “Study of Cellulose Dissolution in ZnO/NaOH/Water Solvent Solution and Its Temperature-Dependent Effect Using Molecular Dynamics Simulation,” *Polymers*, vol. 16, no. 9, pp. 1–12, 2024, doi: 10.3390/polym16091211.  
<https://doi.org/10.3390/polym16091211>
- [13] J. Wang, S. C. Abbas, L. Li, C. C. Walker, Y. Ni, and Z. Cai, “Cellulose Membranes: Synthesis and Applications for Water and Gas Separation and Purification,” *Membranes*, vol. 14, no. 7, pp. 1–34, 2024, doi: 10.3390/membranes14070148.  
<https://doi.org/10.3390/membranes14070148>
- [14] F. P. Morais and J. M. R. Curto, “Design and Engineering of Natural Cellulose Fiber-Based Biomaterials with Eucalyptus Essential Oil Retention to Replace Non-Biodegradable Delivery Systems,” *Polymers*, vol. 14, no. 17, pp. 1–27, 2022, doi: 10.3390/polym14173621.  
<https://doi.org/10.3390/polym14173621>
- [15] A. Nowak, M. Włodarczyk, J. Nawrot, M. Grzeszczuk, M. Ratajczak, B. Kaczmarek, “Bacterial cellulose membrane containing epilobium angustifolium l. Extract as a promising material for the topical delivery of antioxidants to the skin,” *International Journal of Molecular Sciences*, vol. 22, no. 12, pp. 1–21, 2021, doi: 10.3390/ijms22126269.  
<https://doi.org/10.3390/ijms22126269>
- [16] E. Hassan, M. Hassan, R. Abou-zeid, L. Berglund, and K. Oksman, “Use of bacterial cellulose and crosslinked cellulose nanofibers membranes for removal of oil from oil-in-water emulsions,” *Polymers*, vol. 9, no. 9, 2017, doi: 10.3390/polym9090388.  
<https://doi.org/10.3390/polym9090388>
- [17] Y. Sun, X. Qian, Y. Gou, C. Zheng, and F. Zhang, “A Cellulose-Based Dual-Crosslinked Framework with Sensitive Shape and Color Changes in Acid/Alkaline Vapors,” *Polymers*, vol. 16, no. 11, pp. 1–10, 2024, doi: 10.3390/polym16111547.  
<https://doi.org/10.3390/polym16111547>
- [18] J. Vadillo, I. Larraza, T. Calvo-Correas, L. Martin, C. Derail, and A. Eceiza, “Enhancing the Mechanical Properties of 3D-Printed Waterborne Polyurethane-Urea and Cellulose Nanocrystal Scaffolds through Crosslinking,” *Polymers*, vol. 14, no. 22, pp. 1–19, 2022, doi: 10.3390/polym14224999.  
<https://doi.org/10.3390/polym14224999>
- [19] R. Saadan, A. Ihammi, M. Chigr, and A. Fatimi, “A Short Overview of the Formulation of Cellulose-Based Hydrogels and Their Biomedical Applications †,” *Engineering proceedings*, vol. 20, no. 24, pp. 1–12, 2024. doi: 10.3390/engproc2024081003  
<https://www.mdpi.com/2673-4591/81/1/3>
- [20] M. Masruri, U. Z. 'Uyunin, M. Z. Anwar, N. Ikhtiarini, “Citric Acid and Epichlorohydrin as Crosslinking Agent on Hydrogel-Based Cellulose from Pine Cone Flower Potential for Wound Dressing Application,” *Indonesian Journal of Chemistry*, vol. 25, no. 6, p. 1778-1791, 2025, doi: 10.22146/ijc.105566.  
<https://doi.org/10.22146/ijc.105566>
- [21] P. G. Gan, S. T. Sam, M. Omar, and M. F. Abdullah, “Effect of glutaraldehyde as crosslinker on the properties of cellulose nanocrystal/chitosan films,” *IOP Conference Series: Materials Science and*

*Engineering*, vol. 957, no. 1, 2020, doi: 10.1088/1757-899X/957/1/012038. <https://doi.org/10.1088/1757-899X/957/1/012038>

[22] J. G. Jeon, H. C. Kim, R. R. Palem, J. Kim, and T. J. Kang, "Cross-linking of cellulose nanofiber films with glutaraldehyde for improved mechanical properties," *Materials Letters*, vol. 250, pp. 99–102, 2019, doi: 10.1016/j.matlet.2019.05.002. <https://doi.org/10.1016/j.matlet.2019.05.002>

[23] L. O. Mota and I. F. Gimenez, "Cellulose-Based Materials Crosslinked with Epichlorohydrin: A Mini Review," *Revista Virtual de Quimica*, vol. 15, no. 1, pp. 159–170, 2023, doi: 10.21577/1984-6835.20220071. <https://doi.org/10.21577/1984-6835.20220071>

[24] P. Sikdar, Md. M. Uddin, T. M. Dip, S. Islam, Md. S. Hoque, A. K. Dhar, and S. Wu, "Recent advances in the synthesis of smart hydrogels," *Materials Advances*, vol. 2, no. 14, pp. 4532–4573, 2021, doi: 10.1039/d1ma00193k. <https://doi.org/10.1039/d1ma00193k>

[25] H. Nasution, H. Harahap, N. F. Dalimunthe, M. H. S. Ginting, M. Jaafar, O. O. H. Tan, H. K. Aruan, and A. L. Herfananda, "Hydrogel and Effects of Crosslinking Agent on Cellulose-Based Hydrogels: A Review," *Gels*, vol. 8, no. 9, pp. 1–31, 2022, doi: 10.3390/gels8090568. <https://doi.org/10.3390/gels8090568>

[26] M. Janmohammadi, Z. Nazemi, A. Salehi, A. Seyfoori, J. V. John, M.S. Nourbakhsh, M. Akbari, "Cellulose-based composite scaffolds for bone tissue engineering and localized drug delivery," *Bioactive Materials*, vol. 20, no. February 2022, pp. 137–163, 2023, doi: 10.1016/j.bioactmat.2022.05.018. <https://doi.org/10.1016/j.bioactmat.2022.05.018>

[27] N. Ikhtiarini, M. Masruri, S. Mariyah Ulfa, and W. Widodo, "Synthesis and Characterization of Cellulose Acetate and Nanocellulose Acetate from Sengon Agroindustrial Waste (*Paraserianthes falcataria*)," *J. Pure App. Chem Res*, vol. 11, no. 3, pp. 214–224, Dec. 2022, doi: 10.21776/ub.jpacr.2022.011.03.644. <https://doi.org/10.21776/ub.jpacr.2022.011.03.644>

[28] I. A. Udoetok, R. M. Dimmick, L. D. Wilson, and J. V. Headley, "Adsorption properties of cross-linked cellulose-epichlorohydrin polymers in aqueous solution," *Carbohydrate Polymers*, vol. 136, pp. 329–340, Jan. 2016, doi: 10.1016/j.carbpol.2015.09.032. <https://doi.org/10.1016/j.carbpol.2015.09.032>

[29] K. Hettmann, F. W. Monnard, G. Melo Rodriguez, F. M. Hilty, S. Yildirim, and J. Schoelkopf, "Porous Coatings to Control Release Rates of Essential Oils to Generate an Atmosphere with Botanical Actives," *Materials*, vol. 15, no. 6, p. 2155, Mar. 2022, doi: 10.3390/ma15062155. <https://doi.org/10.3390/ma15062155>

[30] S. Hossain, M. A. Jalil, T. Islam, and M. M. Rahman, "A low-density cellulose rich new natural fiber

extracted from the bark of jack tree branches and its characterizations," *Heliyon*, vol. 8, no. 11, p. e11667, Nov. 2022, doi: 10.1016/j.heliyon.2022.e11667. <https://doi.org/10.1016/j.heliyon.2022.e11667>

[31] V. A. Kong, T. A. Staunton, and J. E. Laaser, "Effect of Cross-Link Homogeneity on the High-Strain Behavior of Elastic Polymer Networks," *Macromolecules*, vol. 57, no. 10, pp. 4670–4679, May 2024, doi: 10.1021/acs.macromol.3c02565. <https://doi.org/10.1021/acs.macromol.3c02565>

[32] G. Hoti, F. Caldera, C. Ceccone, A. R. Pedrazzo, A. Anceschi, S. L. Appleton, Y. K. Monfared, and F. Trotta, "Effect of the Cross-Linking Density on the Swelling and Rheological Behavior of Ester-Bridged  $\beta$ -Cyclodextrin Nanosponges," *Materials*, vol. 14, no. 3, p. 478, Jan. 2021, doi: 10.3390/ma14030478. <https://doi.org/10.3390/ma14030478>

[33] A. D. Štiglic, F. Gu'rer, F. Lackner, D. Braccic, A. Winter, L. Gradisnik, D. Makuc, R. Kargl, I. Duarte, J. Plavec, U. Maver M. Beaumont, K. S. Kleinschek, and T. Mohan, "Organic acid cross-linked 3D printed cellulose nanocomposite bioscaffolds with controlled porosity, mechanical strength, and biocompatibility," *iScience*, vol. 25, no. 5, p. 104263, May 2022, doi: 10.1016/j.isci.2022.104263. <https://doi.org/10.1016/j.isci.2022.104263>

[34] J. Liang, R. Wang, and R. Chen, "The Impact of Cross-linking Mode on the Physical and Antimicrobial Properties of a Chitosan/Bacterial Cellulose Composite," *Polymers*, vol. 11, no. 3, p. 491, Mar. 2019, doi: 10.3390/polym11030491. <https://doi.org/10.3390/polym11030491>

[35] L. Yang, Q.-Y. Yuan, C.-W. Lou, T.-T. Li, and J.-H. Lin, "Modified Nanocellulose Hydrogels and Applications in Sensing Fields," *Gels*, vol. 11, no. 2, p. 140, Feb. 2025, doi: 10.3390/gels11020140. <https://doi.org/10.3390/gels11020140>

## 参考文献:

[1] M. Casau, M. F. Dias, J. C. O. Matias, 和 L. J. R. Nunes, "剩余生物质：循环生物经济视角下的重要性、用途及潜力的综合综述", 《Resources》, 第11卷第4期, 第1–16页, 2022年。

<https://doi.org/10.3390/resources11040035>

[2] A. Haryanto 等, "通过热解实现印度尼西亚木材废弃物的高值化利用：综述", 《Energies》, 第14卷第5期, 第1–25页, 2021年。

<https://doi.org/10.3390/en14051407>

[3] I. Rahayu 等, "纳米二氧化硅处理对木豆树木材尺寸稳定性的影响", 《Forests》, 第12卷第11期, 第1–9页, 2021年。 <https://doi.org/10.3390/f12111581>

[4] N. Ikhtiarini 等, "基于纳米纤维素衍生物水凝胶的抗菌性能及其控释应用", 《Tropical Journal of Natural Product Research》, 第8卷第5期, 2024年。

<https://doi.org/10.26538/tjnpr/v8i5.3>

[5] S. Magalhães 等, “纤维素提取与改性的绿色环保方法综述”, 《Polymers》, 第15卷第14期, 第1–25页, 2023年。

<https://doi.org/10.3390/polym15143138>

[6] N. Ikhtiarini 等, “基于海藻酸盐、聚己内酯和纳米纤维素的生物相容复合材料综述”, 《International Journal of Biological Macromolecules》, 第311卷, 143423页, 2025年。

<https://doi.org/10.1016/j.ijbiomac.2025.143423>

[7] R. S. Abolore 等, “木质纤维素生物质中纤维素提取的绿色预处理方法综述”, 《Carbohydrate Polymer Technologies and Applications》, 第7卷, 100396页, 2024年。

<https://doi.org/10.1016/j.carpta.2023.100396>

[8] L. K. Latif 等, “菠萝叶微晶纤维素的制备及其潜力”, 《IOP材料科学与工程会议论文集》, 第833卷, 2020年。 <https://doi.org/10.1088/1757-899X/833/1/012020>

[9] M. Masruri 等, “松木废弃物微晶纤维素的表征研究”, 《AIP会议论文集》, 第2818卷, 2023年。

<https://doi.org/10.1063/5.0131197>

[10] S. Plakantonaki 等, “农业废弃物制备纤维素纤维的上循环路径研究”, 《ChemEngineering》, 第8卷第6期, 第1–32页, 2024年。

[11] J. A. Okolie 等, “木质纤维素生物质的化学特性及工业应用”, 《Waste and Biomass Valorization》, 第12卷第5期, 第2145–2169页, 2021年。

<https://doi.org/10.1007/s12649-020-01123-0>

[12] L. Bourassi 等, “ZnO/NaOH体系中纤维素溶解机理研究”, 《Polymers》, 第16卷第9期, 第1–12页, 2024年。 <https://doi.org/10.3390/polym16091211>

[13] J. Wang 等, “纤维素膜的合成及其在水气分离中的应用”, 《Membranes》, 第14卷第7期, 第1–34页, 2024年。

<https://doi.org/10.3390/membranes14070148>

[14] F. P. Morais 和 J. M. R. Curto, “基于天然纤维素材料的精油控释系统设计”, 《Polymers》, 第14卷第17期, 第1–27页, 2022年。

<https://doi.org/10.3390/polym14173621>

[15] A. Nowak 等, “含植物提取物的细菌纤维素膜用于抗氧化递送”, 《International Journal of Molecular Sciences》, 第22卷第12期, 第1–21页, 2021年。 <https://doi.org/10.3390/ijms22126269>

[16] E. Hassan 等, “交联纤维素膜在油水分离中的应用”, 《Polymers》, 第9卷第9期, 2017年。

<https://doi.org/10.3390/polym9090388>

[17] Y. Sun 等, “双交联纤维素材料对气体响应性能研究”, 《Polymers》, 第16卷第11期, 第1–10页, 2024年。 <https://doi.org/10.3390/polym16111547>

[18] J. Vadillo 等, “交联对3D打印纤维素复合材料性能的影响”, 《Polymers》, 第14卷第22期, 第1–19页, 2022年。

<https://doi.org/10.3390/polym14224999>

[19] R. Saadan 等, “纤维素基水凝胶及其生物医学应用综述”, 《Engineering Proceedings》, 第20卷, 2024年。

<https://doi.org/10.3390/engproc2024081003>

[20] M. Masruri 等, “柠檬酸与环氧氯丙烷交联纤维素水凝胶用于创伤敷料”, 《Indonesian Journal of Chemistry》, 第25卷第6期, 2025年。

<https://doi.org/10.22146/ijc.105566>

[21] P. G. Gan 等, “戊二醛交联对纤维素纳米晶膜性能的影响”, 《IOP会议论文集》, 第957卷, 2020年。 <https://doi.org/10.1088/1757-899X/957/1/012038>

[22] J. G. Jeon 等, “纤维素纳米纤维膜交联改性研究”, 《Materials Letters》, 第250卷, 第99–102页, 2019年。

<https://doi.org/10.1016/j.matlet.2019.05.002>

[23] L. O. Mota 和 I. F. Gimenez, “环氧氯丙烷交联纤维素材料综述”, 《Revista Virtual de Química》, 第15卷第1期, 第159–170页, 2023年。

<https://doi.org/10.21577/1984-6835.20220071>

[24] P. Sikdar 等, “智能水凝胶合成进展”, 《Materials Advances》, 第2卷第14期, 第4532–4573页, 2021年。 <https://doi.org/10.1039/d1ma00193k>

[25] H. Nasution 等, “交联剂对纤维素水凝胶性能的影响综述”, 《Gels》, 第8卷第9期, 第1–31页, 2022年。 <https://doi.org/10.3390/gels8090568>

[26] M. Janmohammadi 等, “纤维素基复合支架在组织工程中的应用”, 《Bioactive Materials》, 第20卷, 第137–163页, 2023年。

<https://doi.org/10.1016/j.bioactmat.2022.05.018>

[27] N. Ikhtiarini 等, “木豆树废弃物制备纤维素衍生物研究”, 《J. Pure App. Chem Res》, 第11卷第3期, 第214–224页, 2022年。

<https://doi.org/10.21776/ub.jpacr.2022.011.03.644>

[28] I. A. Udoetok 等, “交联纤维素吸附性能研究”, 《Carbohydrate Polymers》, 第136卷, 第329–340页, 2016年。

<https://doi.org/10.1016/j.carbpol.2015.09.032>

[29] K. Hettmann 等, “多孔涂层控制精油释放研究”, 《Materials》, 第15卷第6期, 2155页, 2022年。

<https://doi.org/10.3390/ma15062155>

[30] S. Hossain 等, “天然纤维的提取与表征研究”, 《Heliyon》, 第8卷, e11667, 2022年。

<https://doi.org/10.1016/j.heliyon.2022.e11667>

[31] V. A. Kong 等, “交联均匀性对聚合物性能影响”, 《Macromolecules》, 第57卷第10期, 第4670–

4679页，2024年。

<https://doi.org/10.1021/acs.macromol.3c02565>

[32] G. Hoti 等, “交联密度对材料性能的影响”, 《Materials》, 第14卷第3期, 478页, 2021年。

<https://doi.org/10.3390/ma14030478>

[33] A. D. Štiglic 等, “3D打印纤维素复合材料研究”, 《iScience》, 第25卷, 第104263页, 2022年。

<https://doi.org/10.1016/j.isci.2022.104263>

[34] J. Liang 等, “交联方式对复合材料性能影响”, 《Polymers》, 第11卷第3期, 491页, 2019年。

<https://doi.org/10.3390/polym11030491>

[35] L. Yang 等, “改性纳米纤维素水凝胶及其传感应用”, 《Gels》, 第11卷第2期, 140页, 2025年。

<https://doi.org/10.3390/gels11020140>

### Manuscript Information

Word count: 7,253 words (excluding references).

### Peer-Review Record

Fast-track status: Not fast-tracked.

First-round reviews received: 3 reports.

Revision cycles completed: 3 rounds.

Final version submitted: March 24, 2026

### Disclaimer / Publisher's Note

The statements, opinions, and data contained in this article are solely those of the authors and do not necessarily represent the views of the *Journal of Hunan University (Natural Sciences)* or its editorial team. The journal and its editors disclaim any responsibility for injury to persons or property resulting from any ideas, methods, instructions, or products referred to in the content of this article.